

# Detecting and polarizing nuclear spins with double resonance on a single electron spin

P. London,<sup>1</sup> J. Scheuer,<sup>2</sup> J.-M. Cai,<sup>3</sup> I. Schwarz,<sup>3</sup> A. Retzker,<sup>4</sup> M.B. Plenio,<sup>3</sup> M. Katagiri,<sup>5,6</sup> T. Teraji,<sup>6</sup> S. Koizumi,<sup>6</sup> J. Isoya,<sup>5</sup> R. Fischer,<sup>1</sup> L. P. McGuinness,<sup>2</sup> B. Naydenov,<sup>2</sup> and F. Jelezko<sup>2</sup>

<sup>1</sup>Department of Physics, Technion, Israel Institute of Technology, Haifa, 32000, Israel

<sup>2</sup>Institut für Quantenoptik, Universität Ulm, 89073 Ulm, Germany

<sup>3</sup>Institut für Theoretische Physik, Albert-Einstein Allee 11, Universität Ulm, 89069 Ulm, Germany

<sup>4</sup>Racah Institute of Physics, The Hebrew University of Jerusalem, Jerusalem, 91904, Israel

<sup>5</sup>Graduate School of Library, Information and Media Studies,

University of Tsukuba, 1-2 Kasuga, Tsukuba, Ibaraki 305-8550, Japan

<sup>6</sup>National Institute for Materials Science, Tsukuba, Ibaraki 305-0044, Japan

We report the detection and polarization of nuclear spins in diamond at room temperature by using a single nitrogen-vacancy (NV) center. We use Hartmann-Hahn double resonance to coherently enhance the signal from a single nuclear spin while decoupling from the noisy spin-bath, which otherwise limits the detection sensitivity. As a proof-of-principle we: (I) observe coherent oscillations between the NV center and a weakly coupled nuclear spin, (II) demonstrate nuclear bath cooling which prolongs the coherence time of the NV sensor by more than a factor of five. Our results provide a route to nanometer scale magnetic resonance imaging, and novel quantum information processing protocols.

PACS numbers: 67.30.hj, 76.70.Fz, 03.67.Lx, 76.30.Mi, 76.90.+d

Measurements of nuclear spin moments are essential to numerous fields including medicine [1], chemistry [2], metrology [3], and quantum information processing (QIP) [4]. Within these, detection and manipulation of single or few nuclear spins may revolutionize microscopy of biological systems with the possibility to reveal the structure of single molecules. Moreover, the potential of single nuclear spins as long-lived quantum memory units is of intense current interest [5].

However, measurements on single or small ensembles ( $<10^3$ ) of nuclear spins are extremely challenging due to the small nuclear magnetic moment, leading to typically low polarizations, especially at room temperature. Essentially, one must employ a probe close enough to establish the required sensitivity, since the coupling of the probe and the target spin decreases with the distance between them. So far these have only been achieved with magnetic resonance force microscopy [6], quantum dots [7], and recently with the nitrogen-vacancy (NV) center in diamond [8, 9]. The NV center is an attractive system for this task: its optical polarization and spin-dependent photoluminescence along with long ground-state coherence time, make it a perfect probe for sensing nuclear spins coupled to it via dipole-dipole interaction [10].

As the large background noise originating from the spin-bath makes dynamical decoupling techniques a necessity [11], the optimal way to uncover the target signal is not yet fully clear. Recently, three studies have demonstrated the use of pulsed dynamical decoupling to isolate the signal of a single nuclear spin from the nuclear bath [12–14]. Other complementary techniques, applied to small ensembles, have observed statistical fluctuations of nuclear spin states [15, 16]. These signals can be greatly enhanced by hyperpolarization of the nuclei, if such is at disposal.

Here we experimentally show that one can use *continuous dynamical decoupling* (CDD) [17–19] to overcome both challenges, namely to separate a single nuclear spin

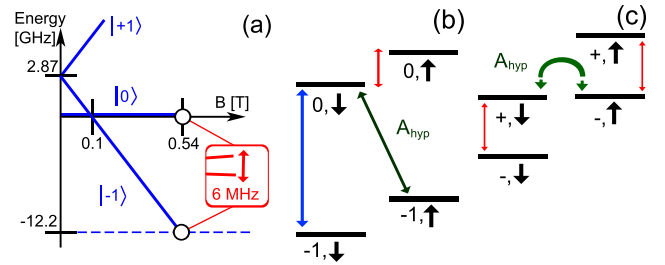


FIG. 1: (color online) (a) Ground-state energy level structure of the NV center as a function of an axial magnetic field. At a magnetic field of 0.54 T, the NV center ground states  $m_s=0, -1$  have an energy separation of 12 GHz, and the nuclear system is split by 6 MHz (Red box). (b) Energy-level diagram of the NV center electronic ground-state and a single  $^{13}\text{C}$  nuclear spin. The coupling term,  $A_{\text{hyp}}$ , induces flip-flops between the electron spin and a coupled nuclear spin (green arrow), which are suppressed by the mismatch of the electronic and nuclear energies (blue and red arrows, respectively). (c) The energy level diagram in the presence of a resonant MW field. The electronic spin is described with the dressed states  $|\pm\rangle$ . At HHDR, coherent oscillations between the  $|+\rangle, \downarrow$  level and the  $|-\rangle, \uparrow$  level (green curve) are enhanced.

signal from the bath noise, and to actively enhance the nuclear polarization of the surrounding bath. In CDD, one applies a continuous, resonant field to isolate the driven spin sensor from its environment. The sensor spin is then insensitive to the surrounding spins, however specific frequency components can be selected through a phenomenon known in nuclear magnetic resonance as Hartmann-Hahn double resonance (HHDR) [19, 20]. We use this technique to experimentally implement an imaging scheme recently proposed in reference [19]. We further demonstrate that CDD can be used (through the spin-locking sequence [2]), to enable direct polarization of the target nuclei [21, 22].

HHDR occurs when two spins with distinct energy sep-

aration are simultaneously driven so that their oscillation (Rabi) frequencies become resonant, or alternatively, when one species is driven with a Rabi frequency that is equal to the energy scale of the other spin [20]. Polarization exchange between the two spin systems can then occur via cross-relaxation, which is usually suppressed by their energy mismatch. In our experiments, corresponding to the latter case, we drive a single NV electronic spin with a Rabi frequency that matches the Zeeman energy of a nearby nuclear spin. This enhances the coherent exchange interaction between the two spins, which would otherwise be prohibited due to the three orders of magnitude energy difference (Fig. 1a,b). By adjusting the intensity of the driving field, the NV spin sensor can be used as a tunable, narrow-band spectrometer [19], with spectral resolution limited only by the decoupling efficiency and interrogation time.

*Hartmann-Hahn dynamics with a single NV-center.* We consider an NV electronic spin,  $\mathbf{S}$ , and an additional  $^{13}\text{C}$  nuclear spin,  $\mathbf{I}$ , with gyromagnetic ratio  $\gamma_N$ . Their interaction can be described by the dipole-dipole term  $H_{NV-^{13}\text{C}} = S_z \cdot \mathbf{A}_{\text{hyp}} \cdot \mathbf{I}$ , where  $\mathbf{A}_{\text{hyp}}$  is the hyperfine vector (see [19, 23]), and non-secular terms are neglected due to the energy mismatch of the two spins (Fig. 1a,b). In an external magnetic field  $\mathbf{B}$ , the splitting between the nuclear states  $|\uparrow\rangle, |\downarrow\rangle$  is  $\gamma_N |\mathbf{B}_{\text{eff}}| = \gamma_N |\mathbf{B} - (1/2) \mathbf{A}_{\text{hyp}}|$  (Fig. 1b, red arrow). If a continuous microwave (MW) field resonant with the  $m_s = 0, -1$  transition, and whose intensity induces Rabi frequency,  $\Omega$ , is applied, the NV center can be described by the MW-dressed states  $|\pm\rangle = \frac{1}{\sqrt{2}}(|0\rangle \pm |-1\rangle)$ . The energy gap of these states is  $\Omega$ , and an energy matching condition (the Hartmann-Hahn condition) given by

$$\delta\Omega = \Omega - \gamma_N |\mathbf{B}_{\text{eff}}| = 0, \quad (1)$$

can be engineered. Then, the energy of the  $|+, \downarrow\rangle$  state and the  $|-, \uparrow\rangle$  state is equal, and being coupled, they will evolve coherently together. The remaining states  $|+, \uparrow\rangle$  and  $|-, \downarrow\rangle$  are separated by  $2\Omega$  (Fig 1c, red arrows), thus decoupled from the joint dynamics. The probability of finding the dressed NV center, initially set to the state  $|+\rangle$ , in the opposite state  $|-\rangle$ , after time  $\tau$ , is

$$p(\tau, \delta\Omega) = \frac{J^2}{J^2 + \delta\Omega^2} \times \sin^2 \left( \sqrt{J^2 + \delta\Omega^2} \frac{\tau}{2} \right), \quad (2)$$

where  $J$ , given by

$$J = \frac{1}{4} \gamma_N |\mathbf{A}_{\text{hyp}}| \sin \theta, \quad (3)$$

is proportional to the coupling strength, and depends on  $\theta$ , the angle between  $\mathbf{B}_{\text{eff}}$  and  $\mathbf{A}_{\text{hyp}}$  (see [23]). The transition probability (Eq. (2)) shows temporal oscillatory behavior, and a spectral dependence (Lorentzian shape of width  $J$ ). The former is a manifestation of the coherent nature of this interaction: starting in the  $|+, \downarrow\rangle$  state, the system evolves according to  $|\Psi\rangle = |+, \downarrow\rangle \cos(Jt) + |-, \uparrow\rangle \sin(Jt)$ . Thus, at time  $t = \pi/2J$  the two spins

become maximally entangled, and after a  $t = \pi/J$  a full population transfer occurs; i.e. the states of the two spins are swapped. The latter spectral dependence in Eq. (2) reflects that coherent oscillations between the NV center and weakly coupled nuclear spins are extremely sensitive to detuning from the Hartmann-Hahn condition.

*Single nuclear spin spectroscopy and imaging.* In our experiments, HHDR is performed with single NV centers in a natural abundance ( $^{13}\text{C}$  1.11%) diamond. (Details on the diamond sample, and on the experimental setup and methods can be found in the supplementary material [23]). In order to increase the decoupling efficiency, we apply a high Rabi frequency of  $\sim 6$  MHz which is matched by the Larmor frequency of the  $^{13}\text{C}$  nuclear spins in a magnetic field of 0.54 T (Fig. 1a). The transition probability in Eq.(2) can be measured in a straightforward way by applying a spin-locking sequence [20, 21]. In this sequence, the NV electronic spin is first optically polarized by 532nm light illumination. Then rotated to the  $|+\rangle$  state with a  $\pi/2$  pulse, and maintained there with a continuous driving field applied at the same frequency, but with a  $90^\circ$  phase shift [23]. Away from HHDR, the NV spin remains in the  $|+\rangle$  state and is subsequently rotated to the low fluorescent,  $|-1\rangle$  state by a final  $\pi/2$  pulse (Fig. 2a). However at the resonance condition, the NV spin undergoes coherent oscillations between the  $|+\rangle$  and  $|-\rangle$  states. After the second  $\pi/2$  pulse this evolution is observed as modulations in the NV fluorescence as the final state oscillates between the  $|0\rangle$  and  $|-1\rangle$  states. As described later, this protocol produces polarization of the nuclear bath, inhibiting further interaction between the NV center and nearby nuclear spins. Therefore, for spectroscopy measurements, i.e characterization of the coupling strength and orientation, an alternating version of the spin-locking sequence was used (Fig. 2b), which produces the same experimental signal but without polarization of the nuclear bath. It comprises two similar sequences “+” and “-”, essentially initializing the NV into the  $|+\rangle$  and  $|-\rangle$  states, respectively. These induce nuclear polarization in alternating directions, thus the net nuclear polarization is zero.

Fig. 2c shows the transition probability of a single NV center interacting with the surrounding spin-bath. Two features which correspond to interaction with nuclear spins can be seen at  $\Omega \simeq 5.76$  MHz and at  $\Omega \simeq 5.9$  MHz. The first agrees well with the expected Larmor frequency for  $^{13}\text{C}$  spins in the applied field ( $|\mathbf{B}| = 5375$  G), and shows loss of coherence of the  $|+\rangle$  state due to the interaction with many nuclear spins. The second feature is the realization of HHDR with a single nuclear spin, whose coupling strength with the NV center ( $\sim 200$  kHz) is 2.5 times smaller than the measured inhomogeneous ( $1/T_2^*$ ) linewidth, which characterizes the phase-detection sensitivity without decoupling. Note, Eq.(2) neglects the NV electronic spin interaction with its host nitrogen nuclear spin ( $^{15}\text{N}$  in this case). For our experimental parameters, HHDR is efficient for a single hyperfine projection which has a time averaged population

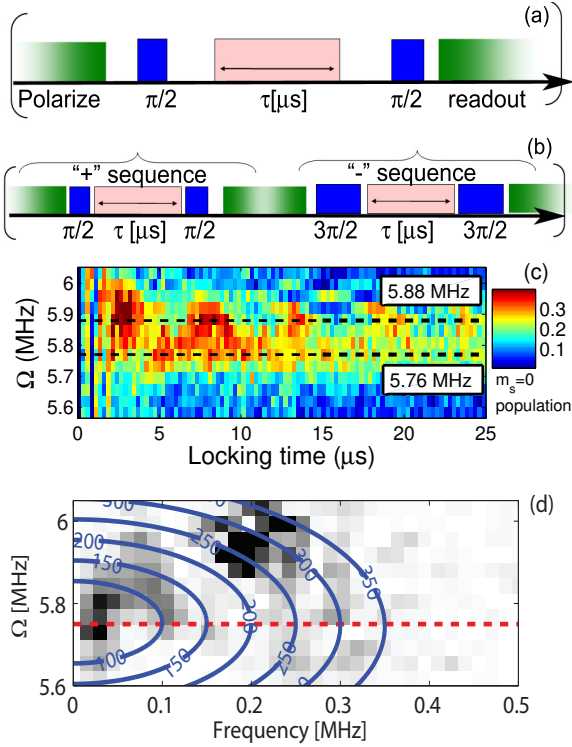


FIG. 2: (Color online) Weakly coupled nuclear spin spectroscopy. (a) The spin-locking sequence; 532nm-light pulses are marked in green, MW pulses in blue and pink, for X and Y pulses, respectively. (b) alternating spin-locking sequence. (c) Experimentally observed population of the  $m_s = 0$  state as a function of the MW driving field  $\Omega$  and the spin-locking time  $\tau$ . Colormap is normalized by the contrast observed in a Rabi experiment (performed with a strong driving,  $\Omega > 13$  MHz). The black dashed lines are guide to the eye. (d) Fourier analysis of the spin-locking signal for various MW driving fields  $\Omega$ . Coupling to a single nuclear spin is apparent as a dark spot around 200 kHz, while coupling to the bath produces the lower frequency signal. The blue lines correspond to the predicted values of the resonance driving amplitude  $\gamma_{13C} |\mathbf{B}_{\text{eff}}|$  (Eq.(1)) and the flip-flop rate  $J$  (Eq.(3)), respectively, for a constant coupling strength and various angles (values are in kHz). The red line is the value of the “bare” Hartmann-Hahn term  $\Omega = \gamma_{13C} |\mathbf{B}|$ .

of 0.45 [23]. Therefore, the 40% oscillation contrast indicates  $\sim 90\%$  polarization exchange efficiency with the single  $^{13}\text{C}$  spin. The two-dimensional nature of Eq. (2), i.e. the spectral and temporal dependencies, also allows for nuclear spin imaging (Fig. 2d). Both the optimal Rabi frequency  $\Omega_{\text{opt}}$  which satisfies Eq. (1), and the oscillation rate at double-resonance (Eq. (3)) contain information about the interaction strength,  $|\mathbf{A}_{\text{hyp}}|$  and its orientation,  $\theta$ . Inverting Eq. (1) and Eq. (3) for this electron-nuclear pair ( $\Omega_{\text{opt}} = 2\pi \times (5.88 \pm 0.03)$  MHz, ( $J = 2\pi \times (188 \pm 30)$  kHz), we deduce that the coupling for this pair is  $(1/4)\gamma_N |\mathbf{A}_{\text{hyp}}| = 2\pi \times 220 \pm 40$  kHz (which corresponds to a nuclear spin located  $\sim 0.5$  nm from the NV center, assuming the contribution from the contact term in the interaction is negligible), and the orientation is  $\theta = 56 \pm 10^\circ$ .

The measured coupling,  $\sim 200$  kHz, does not mark the

ultimate sensitivity of our scheme. Coherent oscillations of the NV-nuclear pair last for more than  $25 \mu\text{s}$ , implying that a 40 kHz coupling could have been detected if such a nuclear spin was present in the vicinity of this NV center, and providing it could be spectrally separated from the spin bath signal at 5.76 MHz ( $\gamma_{13C} |\mathbf{B}|$ ). In principle, the interrogation time and hence the sensitivity of the HHDR scheme, is limited by  $T_1^p$  - the longitudinal relaxation time of the NV center in the rotating frame [2].  $T_1^p$  times exceeding one millisecond have been measured for NV centers at room temperature [24], which translates to sub-kHz resolution. However both practical and fundamental aspects limit the sensitivity of the scheme. First, fluctuations in the applied MW and static magnetic fields cause broadening and reduce the achieved interrogation time. This may be overcome with improved concatenated continuous driving schemes which mitigate the impact of MW instabilities [25]. Second, the decoupling efficiency of CDD depends on the spectral overlap of the environmental noise spectrum with the decoupling filter function [11]. The overlap may be reduced by modifying either the filter function or the bath spectrum to achieve optimal decoupling performance. For example, to target detection of protons [15, 16], the NV-center can be tuned to the proton spectral region, which is detuned from  $^{13}\text{C}$  nuclear spins in moderate magnetic fields. However, in our experiment we aimed to separate the signal of individual  $^{13}\text{C}$  nuclear spins from a bath comprised from the same nuclear species. Then the spectral density of the bath is peaked near the interrogated frequencies (shifted by only the coupling interaction between the sensor and target spin) leading to a reduced  $T_1^p$  coherence time [26]. For a detailed discussion on the sensitivity of the scheme, see [27, 28], and [23].

*Nuclear spin-bath polarization.* In addition to the detection of single or few nuclear spins, one can utilize the direct flip-flops between the NV center and nuclear spins to polarize the surrounding bath (Figure 3). Under HHDR, the  $|+\rangle, |\downarrow\rangle \longleftrightarrow |-\rangle, |\uparrow\rangle$  transition allows transfer of polarization from the NV electronic spin to resonant nuclear spins. Therefore, when optical polarization of the NV spin is established at the beginning of each sweep an efficient cooling mechanism of the nuclear spin-bath is provided. We note that other transitions between the dressed-electronic spin and the nuclear spin can lead to a reversal of polarization [23]. However these transitions are suppressed by an energy mismatch described by  $\sim (J/\Omega)^2$ , and in our high-field experiments are of the order  $1 \times 10^{-3}$ . We observe the bath polarization experimentally in the spin-locking signal when employing the non-alternating sequence (Fig. 2a), which shows no oscillations as the system is driven into a non-interacting state in which all the nuclear spins are polarized to their up state [23]. The bath polarization itself can also be directly observed from the free induction decay (FID) signal of the NV center, measured using a Ramsey sequence.

The results show that when the bath is polarized the

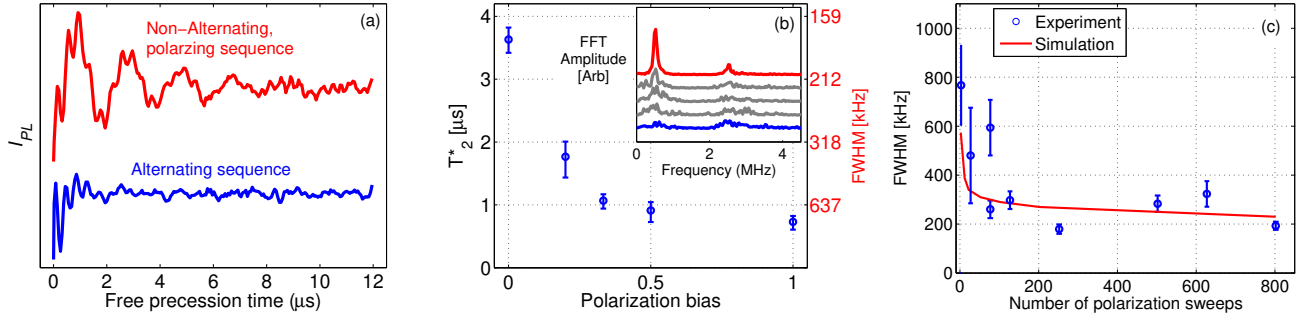


FIG. 3: (color online) Dynamical polarization of the nuclear spin-bath. (a) Free induction decay measured on a single NV center while applying the alternating sequence (blue curve -  $T_2^* \sim 0.6 \mu\text{s}$ ) and while applying the polarization sequence (red curve -  $T_2^* \sim 3 \mu\text{s}$ ). (b) Dependence of the dephasing time  $T_2^*$  on the polarization bias. The inset shows the Fourier amplitudes of the corresponding FID signals, showing a monotonic narrowing as the bias is increased. The lower blue curve and the upper red curves correspond to polarization balance of 1 and 0, respectively, as plotted in Fig. 3a. (c) Build up of the nuclear spin-bath polarization is reflected in a narrowing of the full-width at half-maximum (FWHM) linewidth in the Ramsey measurements as the number of polarization sweeps is increased. The experimental data (circles) qualitatively agree with simulation of direct polarization mechanism under the spin-temperature approximation (red solid line). The simulation includes an additional offset of 150 kHz to account for magnet drifts on the linewidth. In (b),(c) the  $T_2^*$  and FWHM values are extracted by fitting the function  $Y = \Lambda_1 \exp(-((f - \mu_1)/\sigma)^2) + \Lambda_2 \exp(-((f - \mu_2)/\sigma)^2)$  to the Fourier transform spectra (Fig. 3b inset), and by  $\text{FWHM} = 2\sigma\sqrt{\ln 2}$  and  $T_2^* = 2/(\pi \text{ FWHM})$ . The error bars are one standard deviation obtained from the fit process.

NV phase memory time,  $T_2^*$ , increases five-fold in comparison with a non-polarized bath (Fig. 3a). Further improvements in  $T_2^*$  are limited by magnet drifts of our setup. To investigate the polarization dynamics further, the polarization rates towards the up and down state were balanced using  $N_+$  sweeps of the “+” sequence and  $N_-$  sweeps of the “-” sequence. We define the polarization *bias* as  $(N_+ - N_-)/(N_+ + N_-)$ . The smooth transition of  $T_2^*$  times in the range 0.6–3 μs when adjusting the polarization bias from zero to unity indicates that precise control over spin-bath degree of polarization is achievable (Fig. 3b). Finally, we measure the dynamics of the bath polarization by varying the number of polarization sweeps and measure the FID signal (Fig. 3c) [29]. The experimental results are in qualitative agreement with a numerical simulation of a master equation for a single NV center surrounded by 500  $^{13}\text{C}$  spins [30], showing a characteristic gradual polarization. The simulation indicates that close lying nuclear spins are polarized very efficiently (almost one spin per sweep), whereas farther away nuclear spins are polarized much slower [23]. The proximal spins have the greatest influence on the FID linewidth, thus their polarization improves  $T_2^*$  significantly. However this also creates an inherent problem when comparing numerical simulations to the experiment, as both are dependent on the actual configuration of nearby nuclei. Initializing and probing the nuclear-bath state as demonstrated here provides a route for characterizing fundamental processes such as inter-nuclear interactions. For example, it is of great interest to discriminate the aforementioned direct polarization process from spin-diffusion induced polarization process [31].

*Conclusions.* Continuous dynamical decoupling allows a single NV-center to sense minute magnetic fields originating from a single nuclear spin, in spite of the large

background noise produced by its environment. We demonstrated that a careful tuning of the protocol may bring forth room-temperature hyperpolarization among nuclei in the surrounding bath. The interaction between the NV electronic spin and the nuclear spins preserves its coherent nature, i.e. it can support quantum information protocols using dressed qubits [32].

In biological measurements which are characterized with an extremely disruptive environment, CDD can become an optimal tool: First, it allows improved decoupling through high Rabi frequencies at efficient energy expenditure compare to pulsed techniques, and would thus be less invasive to biological samples. Second, using room-temperature nuclear polarization the target spin signal can be amplified, resulting with signal-to-noise ratio improvement according to  $\sqrt{N}$  where  $N$  is the number of nuclear spins. Moreover, for many diamond-based QIP protocols, initialization of the nuclear bath to a given state is essential, for example in quantum simulators [33]. We also note that Hartmann-Hahn double resonance can be applied for the detection of electron spins as was demonstrated recently [34].

The authors thank Rainer Pfeiffer and Kay Jahnke for assistance with the experiments. The authors are grateful to Philip Hemmer, Jörg Wrachtrup, Vyacheslav Dobrovitskii and Philipp Neumann for fruitful discussions. The research was supported by DFG (FOR1482, SPP1601 and SFB TR21), EU (DIAMANT), DARPA (QUASAR) and the Alexander von Humboldt Foundation. J.-M.C acknowledges the support of Marie-Curie fellowship and FP7.



- 
- [1] P. Mansfield, (Nobel Lecture) *Angewandte Chemie International Edition* **43**, 5456 (2004).
- [2] Slichter, C. P. *Principles of Magnetic Resonance*(Springer-Verlag,1990).
- [3] J. H. Simpson, J. T. Fraser, and I. A. Greenwood.IEEE Trans. Aerosp. Support **1**, 1107-1010 (1963).
- [4] P. Neumann et al. *Science* **320**, 1326 (2008).
- [5] Maurer et al. *Science* **336**, 1283-1286 (2012).
- [6] J. A. Sidles et al. *Rev. Mod. Phys.* **67**, 249-265(1995).
- [7] A. Grelich et al. *Science* **317**, 1896-1899 (2007).
- [8] F. Jelezko, T. Gaebel, I. Popa, A. Gruber, and J.Wrachtrup, *Phys. Rev. Lett.* **92**, 076401 (2004).
- [9] L. Childress et al. *Science* **314**, 281-284 (2006).
- [10] M. V. Gurudev Dutt et al., *Science* **316**, 1312-1314 (2007).
- [11] J.M. Taylor et al., *Nature Phys.* **4**, 810-816 (2008).
- [12] S. Kolkowitz, Q.P. Unterreithmeier, S.D. Bennett, and M.D. Lukin, *Phys. Rev. Lett.* **109**, 137601 (2012).
- [13] T. H. Taminiau et al. *Phys. Rev. Lett.* **109**, 137602 (2012).
- [14] N. Zhao et al. *Nature Nanotechnology* **7**, 657 (2012).
- [15] H. J. Mamin, M. Kim, M. H. Sherwood, C. T. Rettner, K. Ohno, D. D. Awschalom, and D. Rugar, *Science* **339**, 557 (2013)
- [16] T. Staudacher, F. Shi, S. Pezzagna, J. Meijer, J. Du, C. A. Meriles, F. Reinhard, and J. Wrachtrup, *Science* **339**, 561 (2013)
- [17] P. Facchi, D. A. Lidar, and S. Pascazio, *Phys. Rev. A* **69**,032314 (2004).
- [18] F. F. Fanchini, J. E. M. Hornos, and R.d.J. Napolitano, *Phys. Rev. A* **75**, 022329 (2007).
- [19] J.M. Cai et al. *New J. Phys.* **15**, 013020 (2013).
- [20] S.R. Hartmann, and E.L. Hahn, *Physical Review* **128**, 5 (1962).
- [21] A. Henstra, P. Dirksen, J. Schmidt, and W. Wenckebach, *J. Magn. Reson.***77**, 389 (1988).
- [22] E. C. Reynhardt et al. *J. Chem. Phys.* **109**, 4100 (1998).
- [23] Supplementary information.
- [24] B. Naydenov et al. *Phys. Rev. B.* **83**, 081201(R)(2011).
- [25] J.M. Cai et al. *New J. Phys.* **14**, 113023 (2012).
- [26] E. van Oort and M. Glasbeek, *Phys. Rev. B.* **40**, 10, 6509 (1989).
- [27] M. Loretz, T. Rosskopf, and C. L. Degen, *Phys. Rev. Lett.* **110**, 017602 (2013)
- [28] M. Hirose, C. D. Aiello, and P. Cappellaro, *Phys. Rev. B.* **86**, 062320(2012).
- [29] To initialize (depolarize) the nuclear bath before each measurement, we have used many sweeps of the alternating sequence.
- [30] H. Christ, J.I. Cirac and G. Giedke, *Phys. Rev. B.* **75**, 155324 (2007).
- [31] R. Fischer et al, <http://arxiv.org/abs/1211.5801> (2012).
- [32] A. Bermudez, F. Jelezko, M. B. Plenio, A. and Retzker, *Phys. Rev. Lett.***107** 150503 (2011)
- [33] J.M. Cai, A. Retzker, F. Jelezko and M.B. Plenio, *Nature Physics* **9**, 168 173 (2013).
- [34] C. Belthangady et al, *Phys. Rev. Lett.* **110**, 157601 (2013).